



Research article

Dysfunctional pericellular hyaluronan deposition contributes to attenuated CD44/EGFR co-localization and impaired myofibroblast differentiation in chronic wound fibroblasts

Nathaniel Glyn Morris^{a,b,c}, Emma Louise Woods^b, Jordanna Dally^b,
Adam Christopher Midgley^{a,d}, Robert Steadman^a, Ryan Moseley^{b,*}

^a Wales Kidney Research Unit, Division of Infection and Immunity, School of Medicine, College of Biomedical and Life Sciences, Cardiff University, Cardiff, UK

^b Disease Mechanisms Group, School of Dentistry, College of Biomedical and Life Sciences, Cardiff University, Cardiff, UK

^c Department of Dietetics, Nutrition and Biological Sciences, Queen Margaret University, Edinburgh, UK

^d The Key Laboratory of Bioactive Materials, Ministry of Education, College of Life Science, Nankai University, Tianjin, China

ARTICLE INFO

Keywords:

Chronic wound
Skin
Fibroblast
Myofibroblast
Differentiation
Hyaluronan
Transforming growth factor- β_1

ABSTRACT

Non-healing chronic wounds, such as venous ulcers and pressure sores, represent significant causes of patient morbidity and financial burden to Healthcare Services worldwide. During normal healing, dermal fibroblasts (DFs) mediate numerous responses to promote wound closure. However, phenotypic changes induced within chronic wound environments lead to dysfunctional fibroblast functions, which facilitate non-healing. Although the processes underlying impaired proliferative and migratory responses in chronic wound fibroblasts (CWFs) are established, the mechanisms that mediate impaired CWF-myofibroblast differentiation remain poorly understood. Fibroblast-myofibroblast differentiation is induced by transforming growth factor- β_1 (TGF- β_1) and downstream classical Smad2/3 and non-classical epidermal growth factor receptor (EGFR)/ERK1/2 signaling, initiated through hyaluronan (HA) receptor (CD44) binding to EGFR and dependent on elevated HA synthesis and its pericellular accumulation. Here, we demonstrate that these signaling pathways are dysregulated in venous ulcer- and pressure sore-derived CWFs, compared to DFs. CWFs exhibit increased susceptibilities to cellular senescence and impaired myofibroblast differentiation, accompanied by defective lysosomal/endosomal activities and dysfunctional activation of the HA/CD44/EGFR pathway. Irrespective of wound source, CWFs exhibited increased HAS1 versus HAS2 expression, altered HAS1 and HAS2 intracellular localization, and deregulated hyaladherin (CD44, TSG-6, and I α I heavy chain motifs, HC3, HC4 and HC5) induction, following TGF- β_1 stimulation. These events attenuated HA pericellular coat formation and CD44/EGFR co-localization within membrane lipid rafts, essential for myofibroblast development. Our findings suggest that aberrant HAS1 and HAS2 expression and distributions cause reduced pericellular hyaluronan deposition, leading to attenuated CD44/EGFR co-localization and dysfunctional CWF-myofibroblast differentiation, which contributes to the impaired closure and healing of chronic wounds.

1. Introduction

Non-healing chronic skin wounds, such as venous leg ulcers (VLUs), diabetic foot ulcers (DFUs) and pressure sores, represent an important source of morbidity in ageing societies and are a significant financial burden to healthcare providers worldwide [1]. Indeed, it has been estimated that it costs healthcare providers in the USA and UK approximately \$96.8 billion and £5.6 billion *per annum* to manage these

wounds, respectively; with wound care costs ever-increasing due to their escalating prevalence because of ever-increasing ageing populations, and obesity and diabetes rates worldwide [2–4].

These wounds are characterized by bacterial biofilm formation and infection, prolonged inflammation, defective extracellular matrix (ECM) turnover and delayed re-epithelialization, enhanced by increased proteolytic remodeling and oxidative stress [5–9]. The consequences of these underlying mechanisms include impaired chronic wound

* Corresponding author. Disease Mechanisms Group, School of Dentistry, College of Biomedical and Life Sciences, Cardiff University, Cardiff, CF14 4XY, UK.

E-mail addresses: Nmorris@qmu.ac.uk (N.G. Morris), WoodsE1@cardiff.ac.uk (E.L. Woods), DallyJ2@cardiff.ac.uk (J. Dally), midgleyac@nankai.edu.cn (A.C. Midgley), SteadmanR@cardiff.ac.uk (R. Steadman), MoseleyR@cardiff.ac.uk (R. Moseley).

<https://doi.org/10.1016/j.yexcr.2025.114646>

Received 12 April 2025; Received in revised form 14 May 2025; Accepted 7 June 2025

Available online 14 June 2025

0014-4827/© 2025 The Authors. Published by Elsevier Inc. This is an open access article under the CC BY license (<http://creativecommons.org/licenses/by/4.0/>).

fibroblast (CWFs) responses, such as reduced proliferation, migration, and growth factor responsiveness, coupled with increased ECM turnover, partly due to increased senescent fibroblast populations in chronic wounds induced via telomere-dependent (replicative senescent) or -independent (stress-induced, premature senescent) mechanisms [10–15].

Fibroblast-myofibroblast differentiation, induced by mediators such as ECM mechanical tension or transforming growth factor- β_1 (TGF- β_1), is a pivotal response in facilitating normal wound closure, contraction, ECM deposition and scar formation [16,17]. However, aberrant myofibroblast activation can result in the development of pathological conditions, such as excessive scarring (fibrosis) and impaired organ function. In contrast, impaired myofibroblast activation leads to non-healing chronic wounds, such as VLU and DFUs [18–20]. Myofibroblasts are characterized by the expression of smooth muscle cell-associated proteins, such as α -smooth muscle actin (α SMA), in addition to a specialized ECM protein, the EDA splice variant of fibronectin (EDA-FN), both of which are regarded as markers of myofibroblast formation and fibrosis [16,17].

During normal TGF- β_1 -mediated, fibroblast-myofibroblast differentiation, TGF- β_1 binds to transmembrane TGF- β receptors (TGF- β R), TGF- β RI and TGF- β RII, leading to type-I receptor recruitment and subsequent heterotetrameric complex formation, which catalyzes type I receptor phosphorylation. Both receptors are essential for activation of the classical TGF- β R signaling pathway, with downstream signaling occurring via Smad2 and Smad3 phosphorylation [16,21]. Our studies, however, have also shown that there is a second synergistic pathway regulating fibroblast-myofibroblast differentiation, without which differentiation is impaired. This synergistic pathway involves the synthesis and pericellular assembly of the ECM glycosaminoglycan, hyaluronan (HA); and its interaction with its principal receptor, CD44 [22–24]. CD44 can also function as a co-receptor for epidermal growth factor receptor (EGFR) and upon TGF- β_1 stimulation, CD44 migrates within the plasma membrane to co-localize with EGFR in lipid rafts [25]. Co-localization also requires a HA-rich environment for HA-CD44 binding, stabilized by tumor necrosis factor-inducible gene 6 protein (TSG-6) and the inter- α -inhibitor (I α) heavy chains, creating a pericellular coat surrounding the cells [26]. The HA/CD44-dependent, EGFR/ERK1/2 pathway has previously been implicated in mediating contrasting wound healing outcomes, due to variations in fibroblast-myofibroblast differentiation responses. For instance, although HA synthase (HAS)2 is responsible for pericellular HA matrix synthesis, oral mucosal fibroblasts that mediate scarless healing *in vivo*, have been shown to be resistant to TGF- β_1 -driven, myofibroblast differentiation [27], associated with an inability to induce HAS2 expression and pericellular HA assembly. Inhibition of HA synthesis in DFs also significantly attenuated TGF- β_1 -mediated, myofibroblast differentiation. Furthermore, loss of HAS2, pericellular HA or the interaction of CD44 with EGFR in aged fibroblasts has also been linked to the attenuation of myofibroblast formation, with overexpression of HAS2 recovering the myofibroblast phenotype [22,24,28,29].

Although dysfunctional proliferation and migration responses in CWFs have been previously well-characterized [13,30–33], to date, no studies have examined the mechanisms underlying the impaired ability of CWFs to undergo TGF- β_1 -driven, myofibroblast differentiation. Therefore, the aim of this study was to assess the hypothesis that defects in the HA-dependent signaling pathways responsible for normal TGF- β_1 -driven, fibroblast-myofibroblast differentiation contributed to dysregulated CWF differentiation and the impaired healing of these wounds.

2. Materials and methods

2.1. Materials

All general and cell culture reagents were purchased from ThermoFisher Scientific (Paisley, UK) or Sigma-Aldrich (Poole, UK), unless

otherwise stated. Real-time quantitative polymerase chain reaction (RT-qPCR) reagents and primers were obtained from ThermoFisher Scientific. Human recombinant TGF- β_1 was sourced from R&D Systems (Abingdon, UK). The primary antibodies and dilutions used for immunocytochemistry were, monoclonal mouse anti- α SMA antibody (1:25), polyclonal rabbit anti-HAS1 (1:200; Abcam, Cambridge, UK), polyclonal goat anti-HAS2 (1:200; Santa Cruz Biotechnology, Dallas, TX, USA), rat monoclonal anti-CD44 (1:200; Merck Millipore, Watford, UK), anti-Hyaluronic Acid Binding Protein (1:100, Merck Millipore), monoclonal mouse anti-EGFR (1:200; Merck Millipore), monoclonal rat anti-EGFR (1:500; Abcam), monoclonal mouse anti-EEA-1 (1:500; BD Biosciences, Wokingham, UK), monoclonal mouse anti-LAMP-1 (1:100; Santa Cruz), monoclonal rabbit anti-calreticulin (1:200; Abcam), monoclonal rabbit anti-GM-130 (1:150; Abcam); and CTX AlexaFluor 555-TRITC (1:1000). The secondary antibodies and dilutions used for immunocytochemistry were, polyclonal goat anti-mouse-IgG AlexaFluor 488-FITC (1:1000), polyclonal goat anti-rat-IgG AlexaFluor 555-TRITC (1:1000), polyclonal donkey anti-goat-IgG AlexaFluor 555-TRITC (1:1000), polyclonal goat anti-rabbit-IgG AlexaFluor 488-FITC (1:1000); and polyclonal goat anti-rabbit-IgG AlexaFluor 555-TRITC (1:1000). The primary and secondary antibodies and dilutions used for Western blot analysis were monoclonal rabbit p-Smad2 (1:1000; Cell Signaling Technology, Cambridge, UK), monoclonal mouse anti-GAPDH (1:2000; Santa Cruz), polyclonal goat anti-rabbit IgG-HRP (1:5000, Abcam); and polyclonal goat anti-mouse IgG-HRP (1:5000; Santa Cruz).

2.2. Cell culture

Primary human non-healing phenotype CWFs and healthy skin-derived dermal fibroblasts (DFs), were sourced from the NIA Aging Cell Respiratory, Coriel Institute (Camden, NJ, USA). CWFs comprised fibroblasts isolated from a venous ulcer (male, 51 years, 3 months' duration wound; AG19285) and a pressure ulcer (male, 35 years, years' duration wound; AG19642). DFs were isolated from two male individuals aged 27 years (GM23962) and 51 years (GM23967). Fibroblasts were cultured in Dulbecco's Modified Eagle's Medium (DMEM) and F-12 Ham Nutrient mixture, containing 5 mM glucose and supplemented with 2 mM L-glutamine, 100 units/mL penicillin, 100 μ g/mL streptomycin and 10 % fetal calf serum (FCS; Biologic Industries Ltd, Cumbernauld, UK). Cells were maintained at 37 °C in a humidified 5 % CO₂/95 % air atmosphere, with medium changed every 72–96 h. At confluence, cells were growth-arrested in serum-free medium for 48 h, before use in experiments. CWFs and DFs were stimulated to undergo myofibroblast differentiation by incubation in serum-free medium containing recombinant TGF- β_1 (10 ng/mL) for 72 h, as previously described [22–24,27]. All experiments were performed under serum-free conditions using equivalent cell numbers, unless otherwise stated.

2.3. Population doubling (PD) analysis and morphological visualization of senescence

CWFs and DFs were expanded in culture throughout their proliferative lifespans, until reaching senescence. At confluence, fibroblasts were detached using trypsin/EDTA and counted using a Coulter Z2 Series Cell Counter (Beckman Coulter, High Wycombe, UK). PD rates were calculated from cell counts throughout their proliferative lifespans and plotted against time in culture, as previously described; with cellular senescence confirmed when fibroblasts underwent <0.5 PDs/week [13]. CWF and DF populations further underwent morphological assessment throughout their proliferative lifespans, with images captured using a Zeiss Axiovert 100M Inverted Microscope (Carl Zeiss Microscopy Ltd, Camburg, UK).

2.4. Immunocytochemistry

Cells were grown to 70 % confluence in 8-well glass chamber slides, growth-arrested for 48 h, and TGF- β_1 stimulated under serum-free conditions. At 72 h, culture medium was removed and the cells washed with sterile phosphate buffered saline (PBS), prior to fixation in 4 % paraformaldehyde (Santa Cruz), for 15 min at room temperature and washing in PBS. Fixed slides were permeabilized with 0.1 % Triton X-100 in PBS for 5 min and immunocytochemistry performed, as previously described [27]. Following mounting (FluorSave, Merck Millipore), slides were analyzed by fluorescence microscopy (Dialux 20 Fluorescent Microscope, Leica Microsystems UK Ltd, Milton Keynes, UK).

2.5. Western blot analysis

Cells were grown in 35 mm dishes, growth-arrested for 48 h, and TGF- β_1 stimulated under serum-free conditions. At the required time-points, cells were washed with ice-cold PBS and total protein contents extracted into RIPA Lysis Buffer, containing 1 % protease inhibitor cocktail, 1 % phenylmethylsulfonyl fluoride and 1 % sodium orthovanadate (Santa Cruz). Protein extracts were separated by sodium dodecyl sulfate-polyacrylamide gel electrophoresis (SDS-PAGE) per manufacturer's instructions, using 7.5 % linear gels and the Mini-PROTEAN II System (Bio-Rad, Hemel Hempstead, UK). Gels were electroblotted onto nitrocellulose membranes (GE Healthcare, Chalfont St. Giles, UK), using a Mini Trans-Blot® Electrophoretic Transfer Cell (Bio-Rad), per manufacturer's instructions. Membranes were blocked with 1 % BSA in 0.1 % Tween/PBS for 1 h at room temperature, and membranes immunoprobed with the appropriate primary antibodies, diluted in 0.1 % Tween/PBS at 4 °C overnight. Normalized protein loading was confirmed using GAPDH as a loading control. Membranes were washed in 0.1 % Tween/PBS and incubated in HRP-conjugated, secondary antibodies for 1 h at room temperature. Membranes were washed in 0.1 % Tween/PBS, incubated in ECL™ Detection Reagent (GE Healthcare) and blots developed using a C-DiGit® Blot Scanner (LI-COR Biotechnology Ltd, Cambridge, UK). Western blot images were analyzed for densitometry, using Image Studio Software (LI-COR).

2.6. Real-time quantitative polymerase chain reaction

RT-qPCR was used to assess the expression of various genes in unstimulated and TGF- β_1 -stimulated DFs and CWFs (Supplementary Tables S1 and S2). Cells were grown in 35 mm dishes, growth-arrested for 48 h, and TGF- β_1 stimulated under serum-free conditions. At 72 h, cells were washed with PBS and total RNA extraction, cDNA generation, amplification and PCR reactions performed as previously described [28, 29], using TaqMan or SYBR Green primer sequences (Supplementary Tables S1 and S2), versus 18S rRNA or GAPDH housekeeping genes, respectively. Relative fold changes in gene expression (RQ) were calculated using the $2^{-\Delta\Delta Ct}$ method [34], normalized versus the housekeeping genes.

2.7. Quantification of hyaluronan levels

Cells were grown to 90–100 % confluence, growth-arrested for 48 h, and TGF- β_1 stimulated under serum-free conditions. Culture media was collected for extracellular HA analysis. Cells were then washed with PBS, followed by treatment with trypsin/EDTA (500 μ L) at room temperature for 5 min to detach pericellular HA; and the trypsin deactivated. The remaining cell layers were collected into Passive Lysis Buffer (500 μ L; Promega, Southampton, UK), for intracellular HA analysis. HA levels were quantified within the separated cell layers by ELISA using HA Test Kits (Corgenix, Peterborough, UK) at 450 nm, according to manufacturer's instructions. Absorbance values were read using a FLUOstar® Omega Plate Reader (BMG Labtech, Aylesbury, UK).

2.8. Hyaluronan pericellular coat formation

Cells were grown to 70 % confluence, growth-arrested for 48 h, and then stimulated under serum-free conditions. At 72 h, cells were washed with PBS and treated with formalized horse blood erythrocytes (TCS Biosciences Ltd, Buckingham, UK), suspended in serum-free medium (1×10^8 cells/mL, 500 μ L/dish), under agitation [27]. Dishes were incubated at 37 °C for 15 min, and zones of erythrocyte exclusion visualized by light microscopy (Zeiss Axiovert 100M Inverted Microscope).

2.9. HAS1 small interfering RNA (siRNA) transfection

Transient transfection of specific siRNA against HAS1 (ID S6454) was used for the targeted downregulation of HAS1 mRNA expression in CWFs. Transfection was performed in 35 mm dishes using Lipofectamine 2000 Transfection Reagent, according to the manufacturer's protocol. Transfection solutions containing Lipofectamine 2000 Transfection Reagent (4 μ L) and OPTI-MEM transfection medium (100 μ L) were prepared, with HAS1 siRNA (30 nM). The solutions were incubated for 40 min at room temperature, before the addition of 800 μ L OPTI-MEM. CWFs were washed with OPTI-MEM and incubated with the transfection solution at 37 °C for 5–7 h, after which additional culture medium (1 mL) containing 20 % FCS was added to the wells. Following 24 h incubation, the medium was removed and replaced with serum-free media, in preparation for further experimentation. As a negative control, CWFs were also transfected with Silencer™ Negative Control No. 1 siRNA (scrambled sequence, ID AM4613). The relative extent of downregulated HAS1 expression in siRNA and scrambled siRNA-transfected CWFs was confirmed by RT-qPCR, as above.

2.10. HAS1 plasmid generation

The HAS1 open-reading frame was inserted into the pCR3.1 vector, using standard ligation with T4 DNA ligase (New England Biolabs, Hitchin, UK). Amplification of the cloned vector was performed via bacterial transformation into one-shot competent, *Escherichia coli* (New England Biolabs), and grown overnight on ampicillin containing agar. Single colonies were extracted, cloned and DNA purified according to the Miniprep Kit protocol [25]. Negative RT experiments were performed alongside HAS1 mRNA RT-qPCR, to ensure that the pCR-3.1-HAS1 was not conveying false-positive overexpression.

2.11. HAS1 overexpression vector transfection

The HAS1 overexpression pCR3.1 plasmid were transfected into CWFs using the Lipofectamine LTX Kit, according to the manufacturer's protocol. Transfections were completed using the Lipofectamine 2000 system, according to the protocol following optimization. Following 24 h incubation, the medium was removed and replaced with serum-free media, in preparation for further experimentation. As a negative control, CWFs were also transfected with an empty pCR3.1 plasmid containing no open reading frame sequence.

2.12. Laser confocal microscopy

Cells were grown to 70 % confluence on sterilized 22 mm diameter glass coverslips in 35 mm dishes, growth-arrested for 48 h, and stimulated under serum-free conditions. At 72 h, cells were fixed and incubated with primary and secondary antibodies, as above. Analysis was performed using Leica Confocal Software, as previously described [28]. Co-localization analysis was performed using a Coloc 2 ImageJ/Fiji Plugin. Images were processed as follows: Split Channels, Subtract Background, and ROI (Green Channel) to provide cell boundaries.

2.13. Statistical analysis

All experiments were performed in triplicate on $n=3$ independent occasions for each DF (A and B) and CWF (VF A and PF B) population analyzed, with data expressed as mean \pm standard deviation (SD). The calculation of Pearson coefficient (r) data for the CD44/EGFR colocalization analysis was undertaken using a Coloc 2 ImageJ/Fiji Plugin, with r values ≈ 1 indicative of a true positive linear correlation between the two variables. Statistical analyses were performed using GraphPad Prism 5 (GraphPad Software, La Jolla, CA, USA). All data were analyzed by two-way Analysis of Variance (ANOVA), with post-Bonferroni test. Significance was considered at $p < 0.05$.

3. Results

3.1. Population doubling (PD) and morphological comparisons of DFs and CWFs

Considering reports that the chronic wound environment can have adverse effects on fibroblast proliferative capabilities due to elevated cellular senescence [10–15], preliminary studies compared the replicative lifespans of venous ulcer- and pressure sore-derived CWFs, versus those of DFs. Analysis of their respective replicative capacities demonstrated that CWFs, such as VLU fibroblasts (VF A) and pressure sore fibroblasts (PF B), exhibited decreased proliferative lifespans and premature senescence, compared to DFs, with VF A and PF B only achieving up to 18PDs (over 100 days in culture) and 12PDs (over 61 days in culture), respectively; prior to senescence (Fig. 1A). In contrast, DF A and B achieved higher PDs without reaching senescence (33–35PDs over 119 and 127 days in culture, respectively). Senescence was further confirmed by fibroblast morphology, with VF A and PF B exhibiting enlarged, stellate morphologies with stress fibers, compared to DF A and B at comparable PDs, which displayed more typical elongated, fibroblastic morphologies (Fig. 1B).

3.2. TGF- β_1 -induced, myofibroblast differentiation in DFs and CWFs

It is well-established that TGF- β_1 stimulation of healthy skin-derived DFs is accompanied by increased α -SMA stress fiber assembly and enlargement in cellular morphology [22–24,27]. Thus, to assess the respective myofibroblast differentiation capabilities of venous ulcer- and pressure sore-derived CWFs, compared to those of DFs, these fibroblast populations were assessed for these myofibroblast markers by immunocytochemistry over 72 h in culture, in the absence and presence of TGF- β_1 stimulation (10 ng/mL). In agreement with our original hypothesis, unstimulated DF (A and B) and CWF (VF A and PF B)

populations exhibited limited α -SMA stress fiber formation and more typical fibroblastic morphologies, although most α -SMA immunostaining present was detectable around the periphery of the cells (Fig. 2A–C and 2E,G). In contrast, TGF- β_1 -stimulated DF A and B displayed positive staining for the presence of α -SMA stress fibers, coupled with a larger, polygonal morphology, confirming phenotypic changes during DF-myofibroblast transition (Fig. 2B–D). However, α -SMA stress fiber formation was severely limited in VLU fibroblasts (VF A) following TGF- β_1 activation, with the fibers irregularly located particularly around the cell periphery (Fig. 2F, red arrows). Additionally, pressure ulcer fibroblasts (PF B) did not induce α -SMA stress fiber formation at all, with α -SMA remaining accumulated around the nucleus (Fig. 2H, white arrows).

Real-time quantitative PCR (RT-qPCR) analysis of α -SMA mRNA expression, confirmed that both DF A and B showed significant induction of α -SMA expression upon TGF- β_1 treatment ($p < 0.0001$ and $p < 0.01$ versus corresponding unstimulated DF controls respectively, Fig. 2I). However, there were no significant increases in α -SMA expression by VF A or PF B, following TGF- β_1 treatment (both $p > 0.05$). EDA-FN mRNA expression also increased in DF A and B when stimulated with TGF- β_1 ($p < 0.0001$ and $p < 0.01$ versus corresponding unstimulated DF controls respectively, Fig. 2J), although there were no significant increases in EDA-FN expression by VF A or PF B (both $p > 0.05$). Therefore, the data collectively suggested that both CWF populations possessed compromised abilities to undergo extensive myofibroblast differentiation essential to wound contraction and closure [16,17].

3.3. Smad pathway activation in DFs and CWFs

In line with our previous reports that the TGF- β_1 -activated, Smad pathway remains activated in senescent fibroblasts in a similar manner to DFs [28,29], CWFs were generally shown to exhibit comparable TGF- β_1 , Smad2 and Smad3 expression; and Smad2 phosphorylation to DFs, following TGF- β_1 stimulation (Fig. S1A–D and S2A,B); although TGF- β RI expression in CWFs (VF A and PF B) was unresponsive to TGF- β_1 treatment (both $p > 0.05$), in contrast to DF A and B ($p < 0.001$ with TGF- β_1 stimulation). Therefore, the findings collectively suggested that dysfunctional TGF- β_1 signaling and downstream p-Smad2/3 activation were not significant contributors to impaired myofibroblast differentiation in CWFs.

3.4. HA pericellular coat formation and hyaladherin expression in DFs and CWFs

The findings described above implied that the non-classical HA/CD44/EGFR/ERK1/2 signaling pathway may be dysregulated, instead

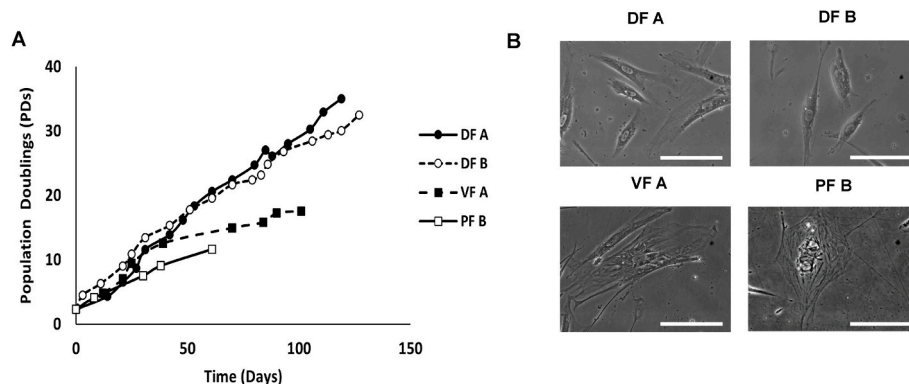


Fig. 1. CWFs exhibit increased susceptibilities to cellular senescence compared to DFs. (A) DFs (A and B) and CWFs (VF A and PF B) were expanded in culture throughout their proliferative lifespans, until reaching senescence. PD rates were calculated from cell counts throughout their proliferative lifespans and plotted against time in culture, with cellular senescence confirmed at <0.5 PDs/week. (B) Assessment of morphological changes associated with senescence development in DFs (A and B) and CWFs (VF A and PF B) throughout their proliferative lifespans.

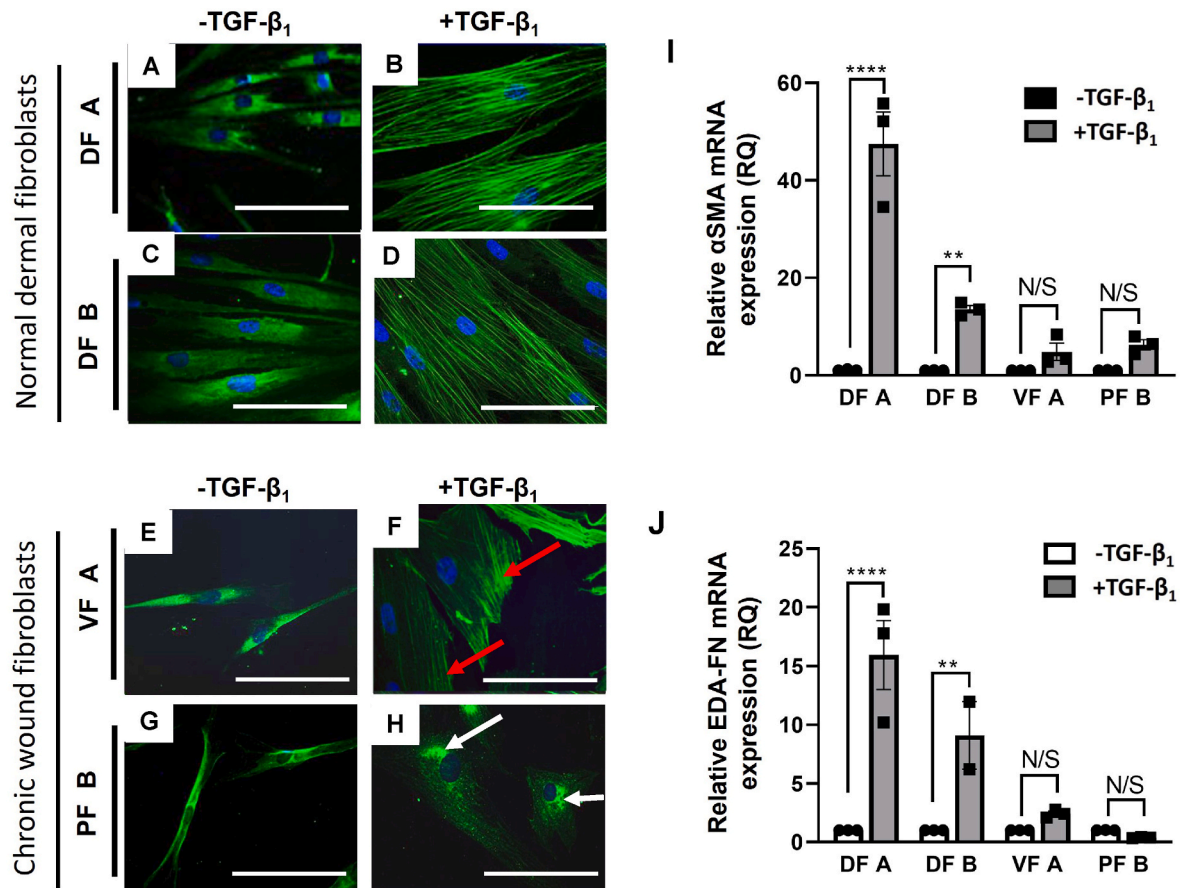


Fig. 2. CWFs display impaired TGF- β_1 -driven fibroblast-myofibroblast differentiation, compared to DFs. Fibroblast-myofibroblast differentiation by (A-D) DFs (A and B) and (E-H) CWFs (VF A and PF B), following stimulation with TGF- β_1 (10 ng/mL) for 72 h, as determined by immunocytochemical analysis of α SMA stress fiber formation. Representative images are shown for three independent experiments. Scale bar = 100 μ m. Relative expressions of myofibroblast markers, (I) α SMA and (J) EDA-FN, as determined by RT-qPCR. Results are shown as mean \pm SD for $n = 3$ triplicates from 3 independent experiments for each DF (A and B) and CWF (VF A and PF B) population analyzed. Significance at $**p < 0.01$, $****p < 0.0001$. N/S, non-significant ($p > 0.05$).

of the classical Smad signaling pathway [28,29]. As part of the non-classical pathway, HAS2 is responsible for the formation of a HA pericellular coat essential for fibroblast-myofibroblast differentiation, whilst removal of the HA pericellular coat or silencing HAS2 expression has been shown to prevent terminal differentiation [22,23,27]. In contrast, HAS1 and HAS3 expression are not associated with HA pericellular coat formation by myofibroblasts [27]. Therefore, it was important to initially investigate the extracellular, cytoplasmic, and pericellular distributions of HA in CWFs and DFs, by ELISA.

Extracellular and cytoplasmic HA was significantly increased in TGF- β_1 -stimulated DF A ($p < 0.0001$ and $p < 0.01$ versus corresponding unstimulated DF controls, respectively; Fig. S3A and B), although no significant increases in HA were determined in either the extracellular or cytoplasmic HA expression between unstimulated and TGF- β_1 -activated DF B, showing variability in HA distribution even in DFs (both $p > 0.05$). Increased extracellular HA was observed by TGF- β_1 -stimulated PF B ($p < 0.01$), but there were no significant increases in extracellular or cytoplasmic HA with VF A or in cytoplasmic HA with PF B (all $p > 0.05$, Fig. S3A and B). In line with previous reports [22,23,27], pericellular HA levels significantly increased in DF A and B, following TGF- β_1 activation (both $p < 0.0001$, Fig. 3A). However, VF A did not demonstrate any significant increases in pericellular HA deposition following TGF- β_1 stimulation ($p > 0.05$), whilst despite a significant increase of pericellular HA being observed in TGF- β_1 -stimulated PF B ($p < 0.05$), this was a more restricted response, compared to the pericellular HA levels formed by DF A and B (Fig. 3A).

Pericellular HA coat formation was further investigated in CWFs and

DFs by erythrocyte exclusion assay, following 72 h TGF- β_1 treatment. DF A and B both displayed extensive HA pericellular coat formation following TGF- β_1 stimulation, compared to unstimulated DF controls (Fig. 3B and C and 3F,G, red arrows). However, there was no HA pericellular coat formation by either VF A or PF B following TGF- β_1 treatment, compared to their unstimulated counterparts (Fig. 3D and E and 3H,I).

HA coats are formed through association with CD44 located on the plasma membrane, and further enhanced by other hyaladherins, such as TSG-6 and I α I heavy chain motifs [22,23,26]. Analysis of CD44 mRNA expression showed no significant differences between unstimulated and TGF- β_1 -stimulated DF A and B, as did PF B (all $p > 0.05$, Fig. 3J). However, significantly decreased CD44 expression was observed in VF A, upon stimulation with TGF- β_1 ($p < 0.05$, Fig. 3J). TSG-6 mRNA also demonstrated no significant differences in expression between normal DF A and B and their TGF- β_1 -treated myofibroblast counterparts (both $p > 0.05$, Fig. 3K). Similarly, there were no significant differences in TSG-6 expression between unstimulated and TGF- β_1 -stimulated PF B ($p > 0.05$), although VF A did show significantly increased TSG-6 expression with TGF- β_1 stimulation ($p < 0.01$, Fig. 3K). As VF A showed dysregulated TSG-6 expression, I α I heavy chain expression were further compared between VF A and DFs. In line with previous findings, HC5 increased in TGF- β_1 -stimulated DFs ($p < 0.0001$) [26], although HC5 failed to exhibit increased expression in VF A, compared to unstimulated controls ($p > 0.05$, Fig. 3L). HC4 also demonstrated increased expression in TGF- β_1 -stimulated DFs ($p < 0.001$, Fig. 3M), although despite HC3 being identified as having limited expression in unstimulated and

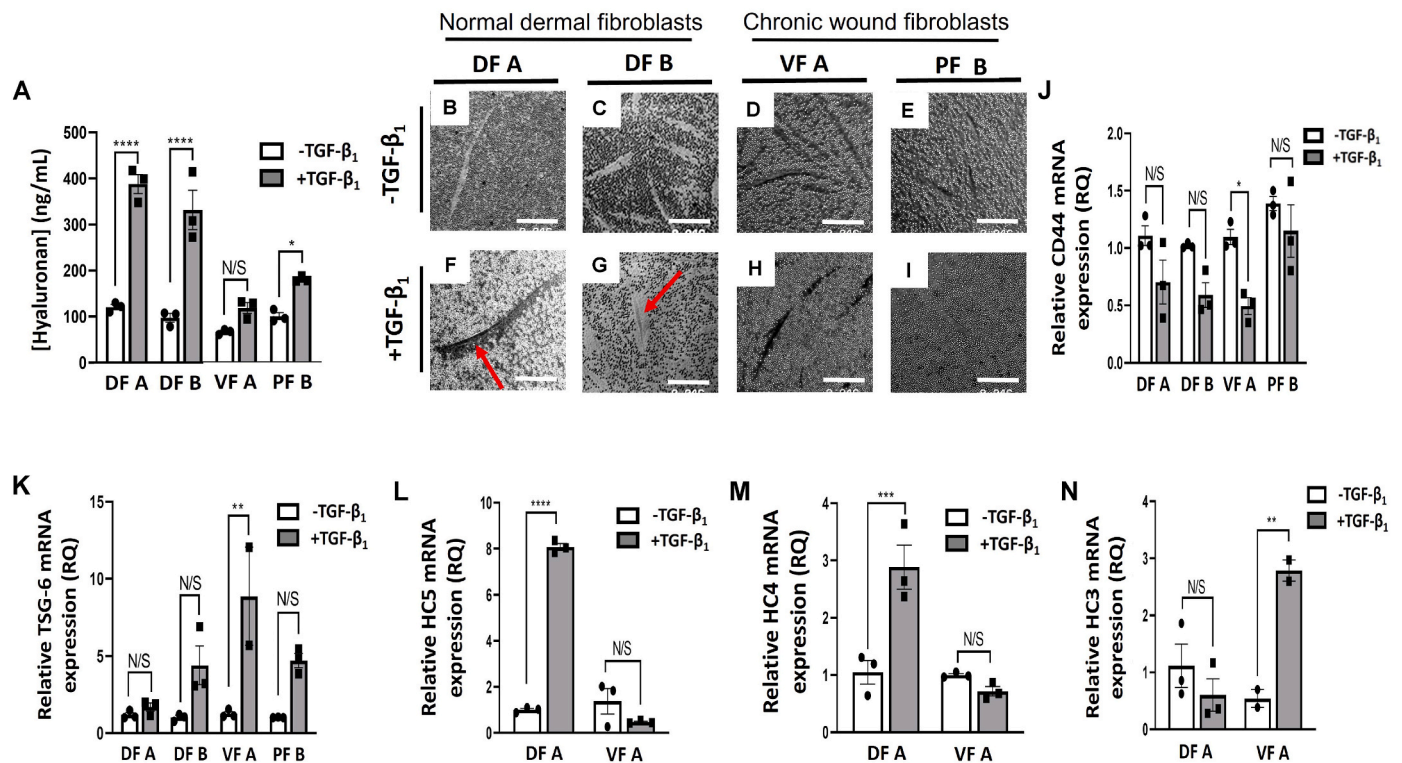


Fig. 3. CWFs exhibit attenuated HA pericellular coat formation and disrupted hyaladherin expression compared to DFs, leading to impaired myofibroblast differentiation. HA pericellular coat formation and hyaladherin expression during fibroblast-myofibroblast differentiation by DFs (A and B) and CWFs (VF A and PF B), following stimulation with TGF- β_1 (10 ng/mL) for 72 h. (A) Quantification of pericellular HA levels by ELISA. HA pericellular coat formation by erythrocyte exclusion assay in (B-E) DFs (A and B) and (F-I) CWFs (VF A and PF B). Representative images are shown for three independent experiments. Scale bar = 100 μ m. Relative expression of hyaladherins, (J) CD44, (K) TSG-6, (L) HC5, (M) HC4, and (N) HC3, as determined by RT-qPCR. Results are shown as mean \pm SD for $n = 3$ triplicates from 3 independent experiments for each DF (A and B) and CWF (VF A and PF B) population analyzed. Significance at * $p < 0.05$, ** $p < 0.01$, *** $p < 0.001$, **** $p < 0.0001$. N/S, non-significant ($p > 0.05$).

TGF- β_1 -stimulated DFs ($p > 0.05$), HC3 expression was significantly upregulated in VF A by TGF- β_1 treatment ($p < 0.01$, Fig. 3N). However, HC1, HC2 and HC6 showed no difference in mRNA expression between DFs and VF A at basal levels or following TGF- β_1 stimulation (Fig. S3C–E).

3.5. HAS1 and HAS2 expression and localization in DFs and CWFs

HAS2 is widely documented to be associated with the HA pericellular coat formation [22,23,27], although this study has shown a distinct failure of HA pericellular coat formation in CWFs treated with TGF- β_1 (Fig. 3). Subsequent RT-qPCR analysis demonstrated that although HAS2 mRNA expression was induced in DF A and B by TGF- β_1 treatment, as with the impeded HAS2 expression response in VF A and PF B following TGF- β_1 -stimulation, these were deemed to be non-significant versus unstimulated DF and CWF controls (all $p > 0.05$, Fig. 4A). In contrast, HAS1 is established to possess no functional role during TGF- β_1 -induced, fibroblast-myofibroblast differentiation [27], and consequently displayed no significant changes in mRNA expression following TGF- β_1 activation in DF A and B (both $p > 0.05$, Fig. 4B). However, VF A and PF B both exhibited major significant increases in HAS1 expression, following TGF β_1 stimulation ($p < 0.001$ and $p < 0.01$, respectively). Nonetheless, in line with previous findings, HAS3 exhibited no significant changes in expression with TGF β_1 treatment in DFs or CWFs (all $p > 0.05$, Fig. S3F). Furthermore, it was confirmed that enhanced hyaluronidase (HYAL1 and HYAL2) expression were not responsible for the reduced pericellular coat formation in CWFs, due to increased hyaluronan catabolism (all $p > 0.05$, Fig. S3G and H) [35,36].

Subsequent studies comparing the localization of HAS1 and HAS2 in CWFs and DFs, identified that HAS2 localization did not alter between

unstimulated and TGF- β_1 -stimulated DFs, with HAS2 diffusely located throughout the cytoplasmic region (Fig. 4C–F for DF A and B, respectively). Similarly, HAS2 was expressed diffusely throughout the cytoplasmic region of VF A. There was also a predominant distribution of HAS2 within the nucleoli of unstimulated VF A (Fig. 4G, white arrow), which increased in VF A following TGF- β_1 stimulation (Fig. 4H, white arrows; enlarged image in Fig. 4I). Interestingly, HAS2 expression was mostly identified within the perinuclear region of PF B, which increased with TGF- β_1 stimulation to form more intense staining in this region (Fig. 4J and K, white arrows; enlarged image in Fig. 4L). Analogous localization studies further identified HAS1 to be present in the nuclear region (blue stain) of unstimulated DFs, which was more diffusely retained within the nuclear region following TGF- β_1 stimulation (Fig. 4M–P for DF A and B, respectively). VF A and PF B also demonstrated perinuclear HAS1 staining in unstimulated fibroblasts (Fig. 4Q–T), but these exhibited increased HAS1 intensities following TGF- β_1 treatment, particularly around the perinuclear regions (Fig. 4R–U; enlarged image in Fig. 4S–V, white arrows).

Therefore, the lack of HA pericellular coat formation by VF A and PF B, coupled with changes in HAS1 expression and intracellular HAS2 and HAS1 localization, collectively suggested that HA is not being formed or distributed correctly in CWFs, as in DFs. Consequently, the intracellular location of HA was compared between DFs and CWFs using immunocytochemistry. HA was present distributed equally throughout the entire cytoplasmic region of unstimulated and TGF- β_1 -stimulated DFs (Fig. 5A and B and 5E,F). However, perinuclear HA accumulation was evident with both unstimulated VF A and PF B (white arrows, Fig. 5C and D), with further increases in perinuclear accumulation with TGF- β_1 treatment (red arrows Fig. 5G and H).

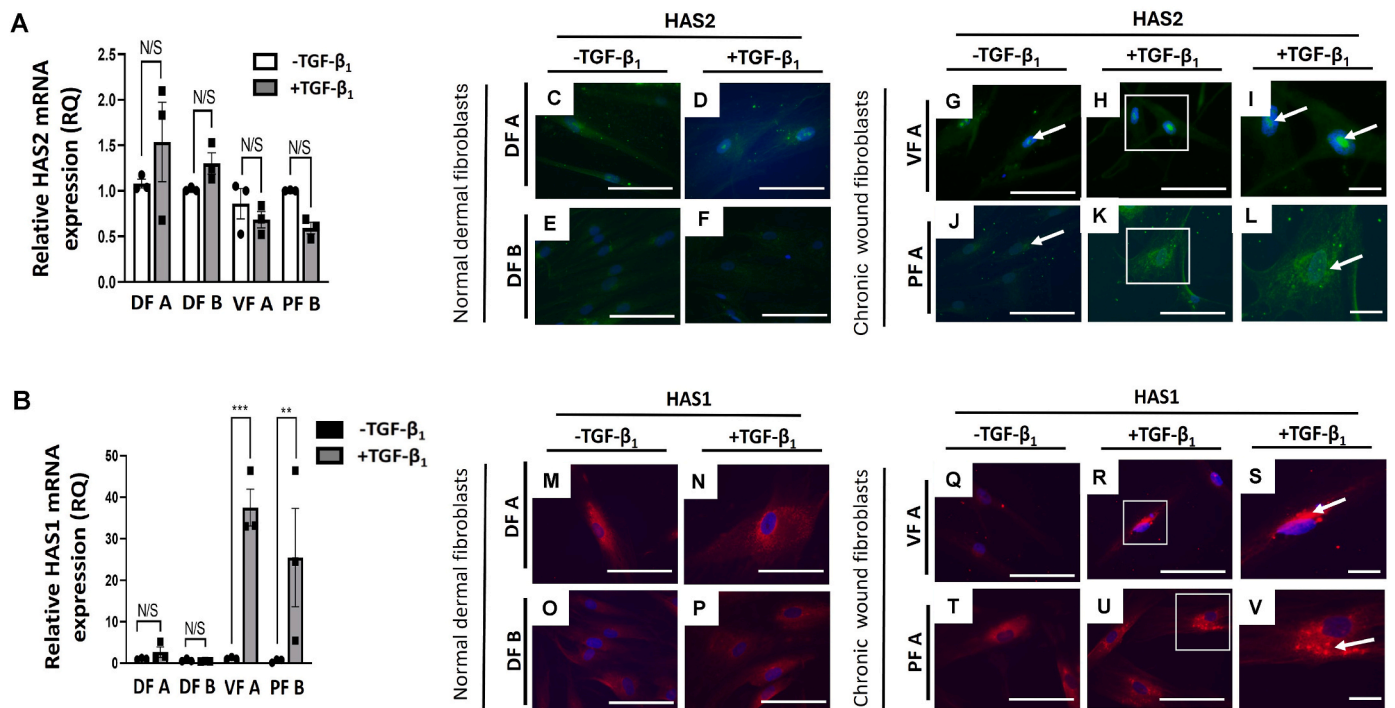


Fig. 4. CWFs show altered HAS1 and HAS2 expression and intracellular localization profiles compared to DFs, contributing to dysfunctional HA pericellular coat formation and myfibroblast differentiation. Expression and intracellular localizations of HAS1 and HAS2 during fibroblast-myofibroblast differentiation by DFs (A and B) and CWFs (VF A and PF B), following stimulation with TGF-β₁ (10 ng/mL) for 72 h. Relative expression of (A) HAS2 and (B) HAS1, as determined by RT-qPCR. Results are shown as mean ± SD for n = 3 triplicates from 3 independent experiments for each DF (A and B) and CWF (VF A and PF B) population analyzed. Significance at **p < 0.01, ***p < 0.001. N/S, non-significant (p > 0.05). HAS2 localization by immunocytochemistry in (C-F) DFs (A and B) and (G-L) CWFs (VF A and PF B). HAS1 localization by immunocytochemistry in (M-P) DFs (A and B) and (Q-V) CWFs (VF A and PF B). Representative images are shown for three independent experiments. Scale bar = 100 μm.

3.6. Effects of manipulating HAS1 gene expression on myofibroblast differentiation

The findings above implicated HAS1 as having a major contribution to the altered HA metabolism and distribution observed in CWFs, such as VF A and PF B, following TGFβ₁ stimulation. Thus, further studies aimed to assess the impact of HAS1 expression on TGF-β₁-induced, myofibroblast differentiation in CWFs and DFs.

Firstly, it was important to determine whether silencing HAS1 expression reestablished myofibroblast phenotype in CWFs, that was lost in VF A and PF B. Transfection of unstimulated CWFs, VFA and PF B, with siRNA decreased HAS1 mRNA expression to ~70 % of that observed in unstimulated non-transfected and negative siRNA-transfected controls. Furthermore, HAS1 siRNA decreased expression by ~ 50 % in TGF-β₁-stimulated CWFs, versus their stimulated negative siRNA-transfected counterparts (Fig. S4A). However, silencing HAS1 mRNA expression in CWFs did not significantly alter αSMA expression or induce αSMA stress fiber formation, compared to CWF controls (Fig. 5I–P). Therefore, silencing HAS1 did not restore the normal myofibroblast phenotype in CWFs.

To further investigate the role of HAS1 in the myofibroblast differentiation process, DFs were subjected to HAS1 vector overexpression, resulting in >50 % HAS1 overexpression in both DF A and B, compared to empty vector transfected DF controls (Fig. S4B). However, HAS1 overexpression induced no significant decreases in αSMA expression or stress fiber formation in DFs (Fig. 5Q–X), versus the empty vector DF controls. Thus, HAS1 overexpression failed to inhibit normal myofibroblast phenotype development in DFs.

3.7. CD44/EGFR co-localization during myofibroblast differentiation in DFs and CWFs

Based on the HAS1 findings above, it can be assumed that the lack of myofibroblast phenotype and loss of HA pericellular coat formation in CWFs, is not solely dependent on dysregulated HA, HAS1 expression or altered intracellular HAS2/HAS1 localization. The TGF-β₁ pathway involved in fibroblast-myofibroblast differentiation is also dependent on the co-localization of principle HA receptor, CD44, with EGFR within lipid-rich regions of the plasma membrane, leading to the downstream activation of ERK1/2 and calmodulin kinase (CAMKII) [25].

Immunocytochemical studies into this essential receptor co-localization found no differences in the expression of CD44 (Fig. 3J) and EGFR (Fig. 6A) between unstimulated DFs and CWFs, with CD44 (red stain) and EGFR (green stain) localized throughout the cytoplasm and the plasma membrane in a comparable manner in both cell types (Fig. 6B–M). Consequently, no CD44/EGFR co-localization were observed in merged images (Fig. 6D–G, J, M; all r values ≥ 0.97), in line with previous reports [25]. However, although no significant difference in CD44 and EGFR expression were shown in TGF-β₁-activated DF A and B, or with PF B (all p > 0.05), significantly decreased CD44 (p < 0.05, Fig. 3J) and EGFR (p < 0.01, Fig. 6A) expression were observed in VF A, following TGF-β₁ treatment. Thus, analysis of CD44/EGFR colocalization in TGF-β₁-stimulated DFs and CWFs, identified that DF A and B displayed increased CD44 (red stain) and EGFR (green stain) association within the plasma membrane (Fig. 6N–S), resulting in completed CD44/EGFR co-localization within the plasma membrane in merged images (white arrows, Fig. 6P–S; both r values ≥ 0.97). In contrast, EGFR was particularly shown to be located within the perinuclear region of TGF-β₁-activated VF A and PF B, with limited EGFR detection in the plasma membrane (Fig. 6T–W). However, despite CD44 demonstrating some association with the plasma membrane in TGF-β₁-treated VF A and

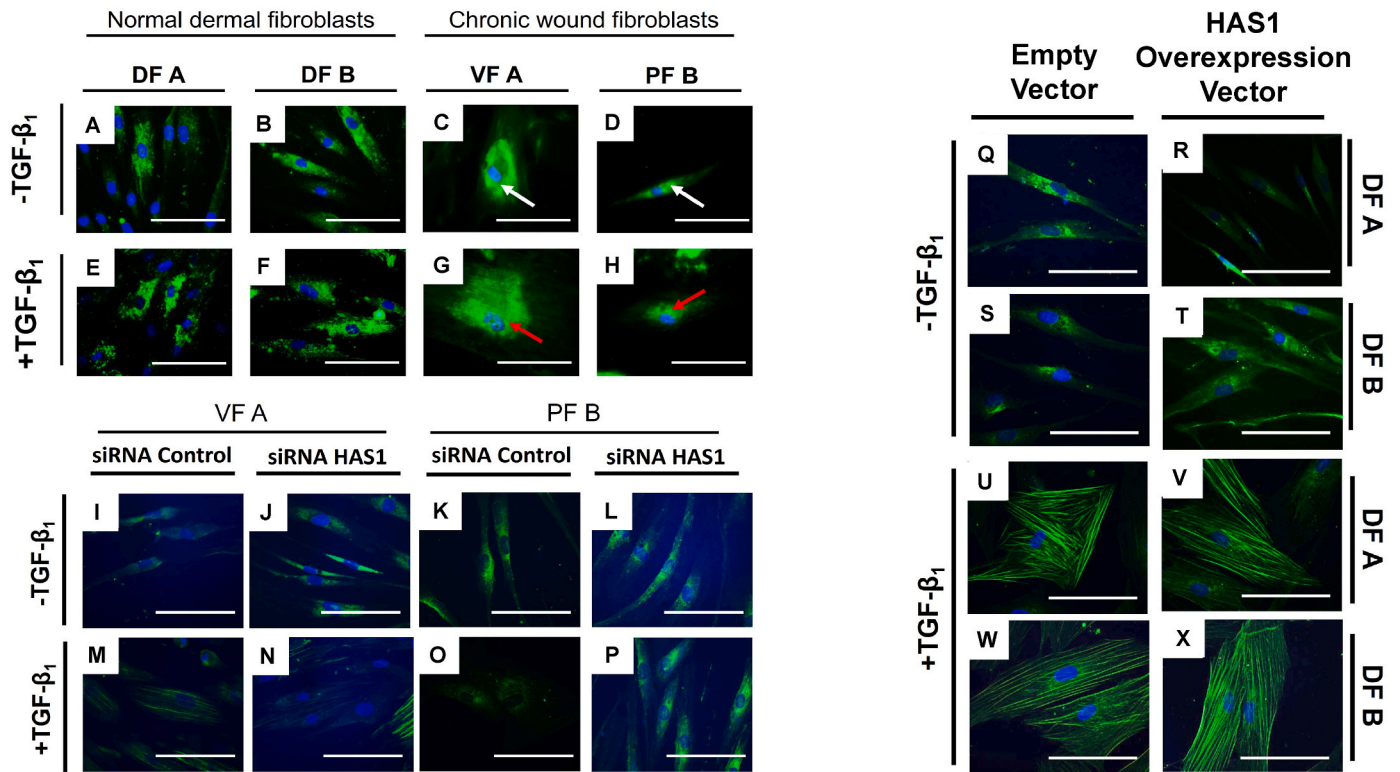


Fig. 5. Altered HAS gene expression and localization profiles cause the dysregulated localization of intracellular HA in CWFs; which cannot be addressed by manipulation of HAS1 gene expression alone. Intracellular HA localization by immunocytochemistry in (A–B, E–F) DFs (A and B) and (C–D, G–H) CWFs (VF A and PF B). HAS1 siRNA effects on fibroblast-myofibroblast differentiation by (I–J, M–N) DFs (A and B) and (K–L, O–P) CWFs (VF A and PF B), following stimulation with TGF- β_1 (10 ng/mL) for 72 h, as determined by immunocytochemical analysis of α SMA stress fiber formation. HAS1 pCR3.1 vector overexpression effects on fibroblast-myofibroblast differentiation by (Q–T) DFs (A and B) and (U–X) CWFs (VF A and PF B), following stimulation with TGF- β_1 (10 ng/mL) for 72 h, as determined by immunocytochemical analysis of α SMA stress fiber formation. Representative images are shown for three independent experiments. Scale bar = 100 μ m.

PF B, this was not as prevalent as the CD44/plasma membrane association observed in TGF- β_1 -stimulated DFs (Fig. 6U–X), with VF A mostly demonstrating perinuclear CD44 localization (Fig. 6U). Therefore, unlike DFs, merged images subsequently identified distinct regions of CD44/EGFR co-localization within the cytoplasm and perinuclear regions in both VF A and PF B following TGF- β_1 stimulation (*white arrows*, Fig. 6V–Y; *r* values of 0.90 and 0.88, respectively), accompanied by the absence of CD44/EGFR co-localization within the plasma membrane. Therefore, confocal images and subsequent co-localization analysis collectively support the disruption of CD44/EGFR colocalization in TGF- β_1 -stimulated CWFs, with EGFR distributed in the cytoplasm rather than in the plasma membrane, contrary to events with TGF- β_1 -treated DFs.

3.8. EGFR/lipid raft association during myofibroblast differentiation in DFs and CWFs

Our previous work identified that during TGF- β_1 -mediated fibroblast-myofibroblast differentiation, CD44/EGFR co-localization within the plasma membrane of myofibroblasts is associated with HA-dependent CD44 transport through the membrane, whilst EGFR remains stationary within the membrane situated within the lipid raft regions [25]. As such CD44/EGFR associations were defective in CWFs, it was necessary to investigate whether a decline in EGFR/lipid raft associations were a potential cause of this dysfunctional response.

Immunocytochemical analysis of EGFR (*green stain*) and lipid raft marker, CTX (*red stain*), showed EGFR and CTX localization throughout the cytoplasm of unstimulated DF and CWFs, with merged images demonstrating no EGFR/CTX colocalization with both cell types (Fig. S5A–L). However, when stimulated with TGF- β_1 , EGFR became

localized within the plasma membrane and cytoplasm of DFs (Fig. 7A–D), although no plasma membrane EGFR was detected with VF A or PF B, being primarily localized within the cytoplasm and perinuclear region (Fig. 7G–J). Similar patterns of CTX localization were also observed, being present within the plasma membrane and cytoplasm of TGF- β_1 -stimulated DFs (Fig. 7B–E), but solely within the cytoplasm of CWFs, VF A and PF B (Fig. 7H–K). Therefore, as previously identified, merged images confirmed that EGFR and CTX co-localized within the plasma membrane in TGF- β_1 -treated DFs, but not in the cytoplasm (*white arrow*, Fig. 7C–F). However, in contrast, EGFR/CTX colocalization was absent from the plasma membrane of TGF- β_1 -stimulated CWFs; but displayed EGFR/CTX colocalization in the cytoplasm (*white arrows*, Fig. 7I–L).

3.9. Intracellular trafficking in DFs and CWFs during myofibroblast differentiation

Based on the CD44/EGFR and lipid raft co-localization findings above, it was important to assess the intracellular trafficking capabilities of DFs and CWFs, to ascertain their potential involvement in mediating impaired myofibroblast differentiation capabilities in CWFs. Endosomes and lysosomes are organelles involved in the sorting, transporting, and degradation of lipids, proteins, and extracellular components of cells [37–39]. Using the lysosome marker, LAMP, lysosome distribution was compared between DFs and CWFs. Unstimulated DFs and CWFs exhibited LAMP localization within the cytoplasmic regions strongly associated with the nuclear region (Figs. S5M, O, Q, S). When stimulated with TGF- β_1 , LAMP distribution in DFs became more diffuse throughout the cytoplasm and less associated with the perinuclear region (Fig. S5N and P). However, LAMP did not show a diffuse cytoplasmic pattern in

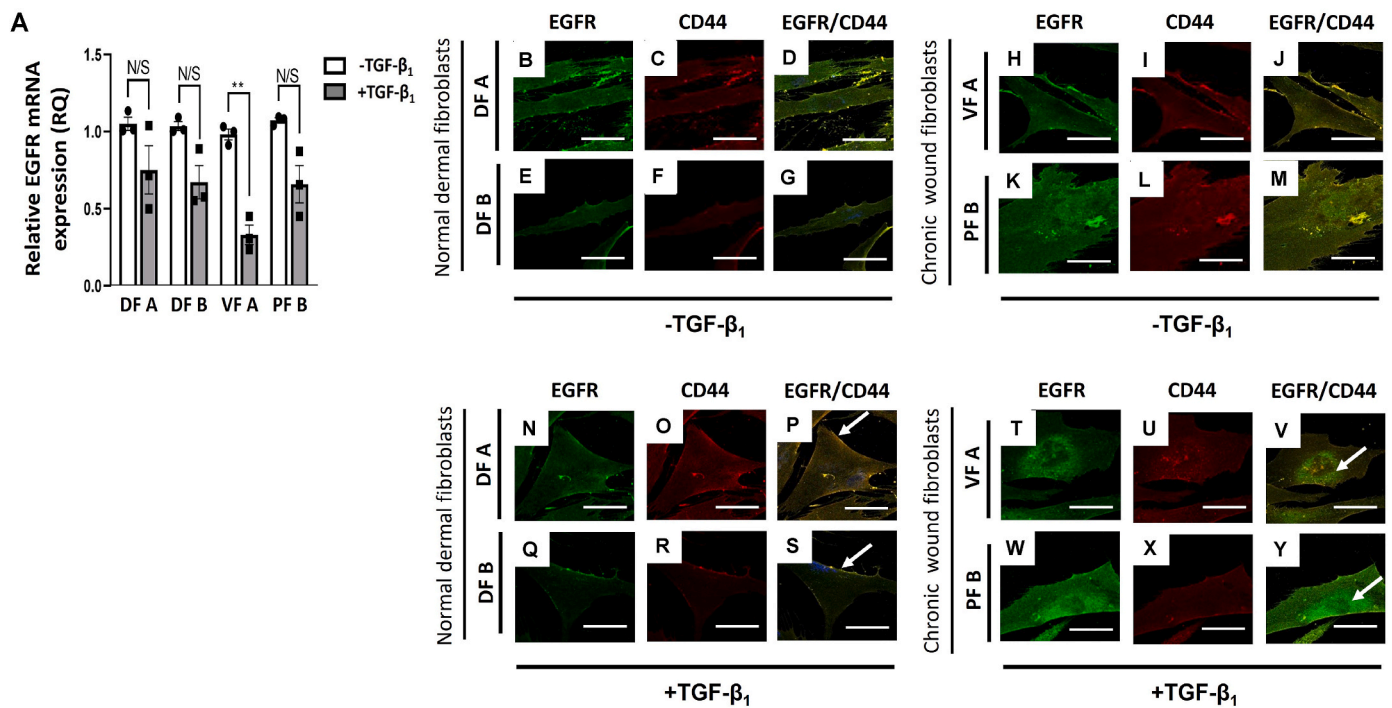


Fig. 6. CWFs exhibit comparable EGFR expression profiles to DFs; but display attenuated CD44/EGFR co-localization in CWFs contributing to impaired myofibroblast differentiation. EGFR expression and CD44/EGFR co-localization during fibroblast-myofibroblast differentiation by DFs (A and B) and CWFs (VF A and PF B), following stimulation with TGF- β_1 (10 ng/mL) for 72 h. Relative expression of (A) EGFR, as determined by RT-qPCR. Results are shown as mean \pm SD for $n = 3$ triplicates from 3 independent experiments for each DF (A and B) and CWF (VF A and PF B) population analyzed. Significance at $^{**}p < 0.01$, N/S, non-significant ($p > 0.05$). EGFR (B, E, H, K, N, Q, T, W), CD44 (C, F, I, L, O, R, U, X), and merged CD44/EGFR co-localization (merged images, D, G, J, M, P, S, V, Y) by immunocytochemistry in (B-G, N-S) DFs (A and B) and (H-M, T-Y) CWFs (VF A and PF B). Representative images are shown for three independent experiments. Scale bar = 100 μ m.

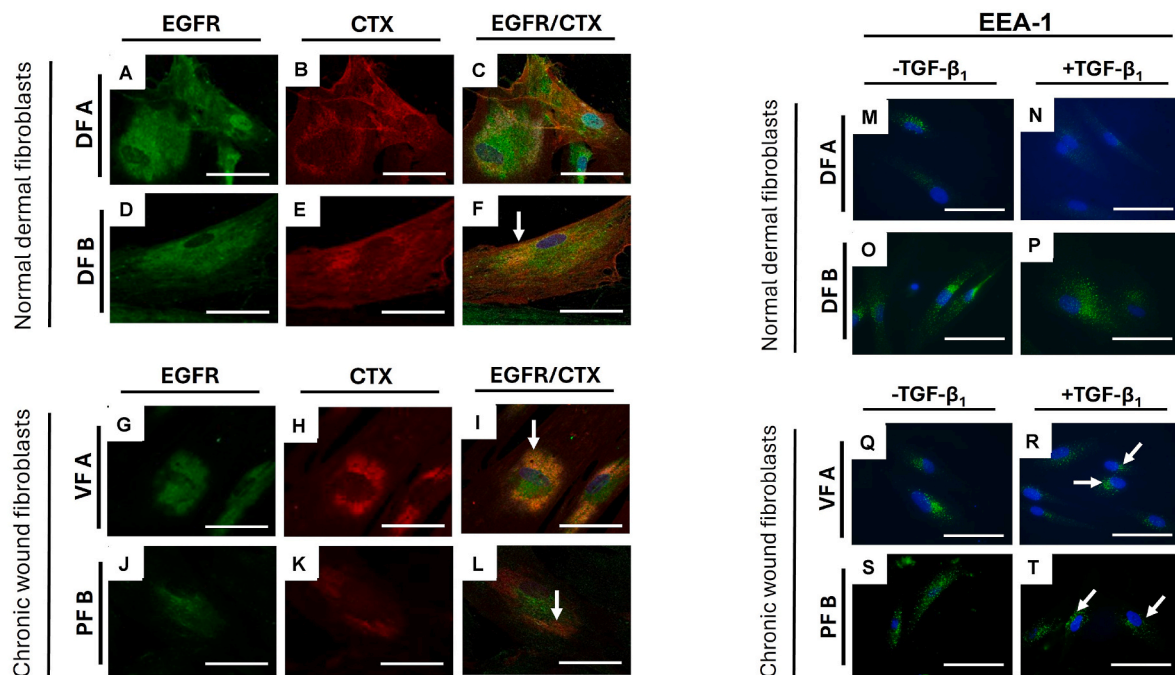


Fig. 7. Impaired downstream EGFR/lipid raft association and defective lysosomal/endosomal activities lead to dysfunctional myofibroblast differentiation in CWFs. EGFR/lipid raft association and EEA-1 localization during fibroblast-myofibroblast differentiation by DFs (A and B) and CWFs (VF A and PF B), following stimulation with TGF- β_1 (10 ng/mL) for 72 h. EGFR (A, D, G, J), CTX (B, E, H, K), and merged EGFR/CTX co-localization (merged images, C, F, I, L) by immunocytochemistry in (A-F) DFs (A and B) and (G-L) CWFs (VF A and PF B). EEA-1 localization by immunocytochemistry in (M-P) DFs (A and B) and (Q-T) CWFs (VF A and PF B). Representative images are shown for three independent experiments. Scale bar = 100 μ m.

TGF- β_1 -stimulated CWFs, being primarily located within the perinuclear region in an equivalent manner to unstimulated CWFs, especially with PF B (Fig. S5R and T).

Early endosome antigen (EEA-1) is associated with the formation of early endosomes, responsible for protein trafficking to and from the plasma membrane [40]. EEA-1 was found to be present throughout the cytoplasm of unstimulated and TGF- β_1 -stimulated DFs (Fig. 7M–P). In contrast, TGF- β_1 -stimulated VFA and PF B showed a closer EEA-1 association with the perinuclear region, comparable to unstimulated CWFs (white arrows, Fig. 7Q–T).

Organelles, such as the endoplasmic reticulum and Golgi apparatus, are responsible for synthesizing, trafficking, and folding proteins [41–43]. Thus, through the detection of endoplasmic reticulum and Golgi apparatus markers, calreticulin and GM-130, we finally explored whether these organelles were defective in CWFs, thereby resulting in the impaired processing, secretion and/or degradation of irregular proteins which may account for the perinuclear accumulation of myofibroblast differentiation mediators in these cells. However, these studies confirmed that there were no detectable differences in the location of these markers between DFs and CWFs, irrespective of being unstimulated or treated with TGF- β_1 (Fig. S6A–H and S6I–P, respectively).

4. Discussion

DFs are key regulators of acute wound healing responses in normal skin, culminating in wound closure, contraction, and scar formation [16, 17,44]. However, it is well-established that the local environment within chronic wounds can have significant deleterious effects on the genotypic and phenotypic responses of fibroblast populations present within the wounded dermis, due to prolonged exposure to contributory factors, such as microbial colonization, biofilm formation and infection; coupled with persistent chronic inflammation [5–9]. Thus, resident CWF within such a pro-microbial/pro-inflammatory milieu leads to their development of defective wound healing capabilities, which perpetuate the non-healing nature of these wounds [13,30–33]. However, whereas impaired proliferative and migratory responses are well-documented, our understanding of how the chronic wound environment influences the ability of CWFs to undergo TGF- β_1 -driven, fibroblast-myofibroblast differentiation, remain relatively unexplored. Therefore, the present study provides key data confirming the dysfunctional myofibroblast differentiation capabilities of CWFs, and the underlying mechanisms involved that potentially contribute to the impaired healing of these wounds.

In line with previous reports [10,12,13], initial studies confirmed that both the venous ulcer- and pressure sore-derived CWFs (VF A and PF B) prematurely exhibited two key hallmark characteristics of *in vitro* cellular senescence compared to DFs; namely reduced replicative lifespans prior to senescence, accompanied by the elevated detection of larger, stellate CWF morphologies. Indeed, despite a degree of heterogeneity existing in the PD capabilities of CWFs derived from different patients, the proliferative lifespans of the CWFs and DFs analyzed in the present study (12–18PDs with VF A and PF B; versus 33–35PDs with DF A and B), were comparable to those previously described from CWFs and DFs in other studies [12,13].

As the chronic wound environment has been suggested to cause dysfunctional proliferative and migratory wound healing activities in CWFs, subsequent studies confirmed that similar impairments in TGF- β_1 -driven, fibroblast-myofibroblast differentiation were evident in CWFs, manifested by significantly reduced inductions in the expression of myofibroblast markers, α SMA and EDA-FN, in addition to α SMA contractile stress fiber formation upon TGF- β_1 stimulation [16,17]. Despite the present study being the first to provide an in-depth investigation into the mechanism associated with impaired myofibroblast differentiation in CWFs, previous studies have confirmed that senescent DF populations also possess an impaired ability to undergo

myofibroblast differentiation *in vitro*, associated with the loss of α SMA/EDA-FN expression and α SMA stress fibers, as evident herein [22, 24,29]. Although CWFs and aged DFs have previously been shown to express elevated levels of endogenous TGF- β_1 expression [12,45], these fibroblast populations also exhibit reduced responsiveness to TGF- β_1 and downstream p-Smad2/3 signaling, due to decreased TGF- β RII expression [11,46–49]. However, concurrent with the data presented here, comparable TGF- β_1 responsiveness and p-Smad2/3 signaling has been reported in young and aged DFs overall [28,29]. Therefore, these findings suggested that although p-Smad2/3 signaling may be partly attenuated in CWFs, it is not entirely defective and as such, dysfunctions in the classical Smad pathway appear not to be extensively involved in the abrogated myofibroblast differentiation responses of CWFs.

Subsequent investigations focused upon unravelling whether dysregulation in components of the non-classical HA/CD44/EGFR pathway were responsible for the impaired fibroblast-myofibroblast responses in TGF- β_1 -stimulated CWFs, initially dependent upon HA pericellular coat formation by HAS2 [22,23,27]. These studies identified that in contrast to usual mechanisms of pericellular HA accumulation and myofibroblast formation in DFs, CWFs were associated with severely diminished HA pericellular coat formation, accompanied by significantly increased HAS1 at the expense of HAS2 expression. However, no changes in HAS3, HYAL1 or HYAL2 expression were determined during the differentiation of TGF- β_1 treated CWFs and DFs, as previously described [27,35,36]. Furthermore, in addition to these alterations in HAS1 and HAS2 expression profiles in CWFs, variations in the intracellular locations of HAS1 and HAS2 were also identified in CWFs, with the prominent perinuclear/nucleoli localization of HAS1 and HAS2, especially following TGF- β_1 stimulation.

Such findings collectively suggested that considerable disruption to the normal mechanisms of HA pericellular coat formation occurred in CWFs, leading to dysfunctional TGF- β_1 -stimulated myofibroblast differentiation; mediated through disturbances in HAS1 and HAS2 gene expression and their intracellular localization. Indeed, as HA pericellular coat formation is highly dependent on the HAS2 isoform, previous studies have confirmed that the removal of the HA pericellular coats or reductions in HAS2 expression significantly inhibits myofibroblast differentiation, as evident in aged DFs [22,24,27]. In contrast, whilst HAS1 is not commonly associated with HA pericellular coat formation in myofibroblasts [27], its upregulated expression has been reported in venous ulcer-derived CWFs, as has its increased expression during chronic inflammation and cellular senescence [13,50,51]. Previous studies have also reported the marked intracellular accumulation of endogenous HA within vesicles in perinuclear regions, associated with enhanced receptor-mediated HA endocytosis in quiescent cells [52]. Similar supporting evidence is derived from HAS1 being shown to produce limited HA pericellular coats dependent on CD44-HA interactions, which orchestrate pro-inflammatory responses [51,53]; whilst HAS1/3 double-knockout mice display significantly faster wound closure, and early onset myofibroblast differentiation and scar formation via activated p38 mitogen-activated protein kinase (MAPK) signaling, than their wild-type counterparts [54,55]. Thus, with HAS1 becoming the predominant isoform present in CWFs, combined with the atypical perinuclear/nucleoli compartmentalization of HAS1 and HAS2 than their locations within the plasma membrane [56], such events may culminate in the subsequent inhibition of HA pericellular coat formation and myofibroblast differentiation in CWFs, due to their dysregulated perinuclear entrapment, as shown herein.

As elevated HAS1 expression and the loss of HA pericellular coat assembly were suggested to contribute to impaired myofibroblast differentiation, we hypothesized that the modulation of HAS1 expression in CWFs and DFs would potentially recover the myofibroblast phenotype in CWFs; or induce a CWF phenotype in DFs. However, both HAS1 silencing and overexpression had no effects on CWF/DF phenotype, in terms of myofibroblast differentiation. These findings demonstrated that HAS1 was not integral to the loss of myofibroblast differentiation in

CWFs and thus, it is elevated expression in TGF- β_1 -treated CWFs may be considered more of a downstream consequence of the chronic wound environment and impaired differentiation, rather than HAS1 having a direct causal effect. Such conclusions would be supported by previous studies demonstrating that neither overexpression nor downregulation of HAS1 in DFs influences myofibroblast differentiation [27], although HAS1/3 double-knockout mice exhibit early onset myofibroblast differentiation and scar formation versus wild-type [54,55]. Similarly, the targeted overexpression of HAS2 in aged DFs have been determined to be resistant to TGF- β_1 -induced, myofibroblast differentiation; implying that other dysfunctional proteins within the non-classical signaling pathway contribute to the loss of differentiation [28]. Thus, similar observations may be the case with HAS1 overexpression in CWFs.

Pericellular matrices consist of hyaluronan interacting with hyaladherins within the ECM, especially CD44, which regulate cellular responses including myofibroblast differentiation [22,23,25,26,28,56]. Our findings demonstrated that unlike pressure-sore-derived, PF B, CD44 and other hyaladherins implicated in the development of the myofibroblast phenotype exhibited differential expression profiles in venous-ulcer-derived, VF A, compared to TGF- β_1 -stimulated DFs. These included significantly decreased CD44 and increased TSG-6 and I α I heavy chain motif, HC3, expression in VF A, coupled with the unresponsive upregulation of I α I heavy chain motifs, HC4 and HC5.

CD44 and these other cell surface hyaladherins are essential for stable HA coat formation during myofibroblast differentiation [22,23,26]. Such events are facilitated by the stabilization of interactions between HA and CD44, particularly aided through interactions between TSG-6 and HC5, as knockdown of expression of either of these hyaladherins inhibits TGF- β_1 -driven myofibroblast formation [26]. Heavy chains and TSG-6 have also been identified to have dysregulated expression which contributes to chronic inflammatory diseases [57]. Thus, although TSG-6 responses were similar in PF B and DFs, the loss of CD44 and HC5 responsiveness in VF A, in addition to elevated TSG-6 expression, could account for the considerable disruption and failure of normal HA pericellular coat assembly in these CWFs.

As part of the non-classical signaling pathway, previous studies have further implicated the downstream loss of EGFR as a primary cause for age-associated impairments in wound healing responses and resistance to myofibroblast differentiation in DFs, leading to impaired CD44 mobility, and reduced CD44/EGFR co-localization within membrane lipid rafts [24,28,29,58]. As described above with CD44, TSG-6 and HC5, EGFR was only downregulated in VF A, but not in PF B or the DFs analyzed, which may suggest that the contrasting etiologies and pathophysiology of distinct types of chronic wound may cause wound-specific alterations in differentiation mediators in CWFs isolated from different wound sources. Nonetheless, as evident in aged fibroblasts, the similar loss of CD44/EGFR co-localization in membrane lipid rafts would be strongly implicated as a reason for the lack of HA pericellular coat formation and subsequent inhibition of myofibroblast formation in CWFs; with data suggesting that the lack of CTX/EGFR co-localization at the plasma membrane in TGF- β_1 -treated CWFs may contribute to the lack of CD44/EGFR plasma membrane association during CWF-myofibroblast differentiation.

As endoplasmic reticulum-Golgi apparatus-plasma membrane trafficking is further essential for HA transfer to the plasma membranes and pericellular coat assembly [59], we next determined that there were no apparent differences in endoplasmic reticulum or Golgi apparatus marker localization between CWFs and DFs. Such findings suggested that protein synthesizing, trafficking, and packaging capabilities remained relatively intact in CWFs [41–43], despite endoplasmic reticulum stress responses being implicated in alterations to DF characteristics during chronic conditions [60,61]. However, using the lysosome and early endosome markers, LAMP and EEA-1, lysosomes and endosomes were shown to be primarily localized within the perinuclear regions of unstimulated and TGF- β_1 -treated CWFs, in contrast to the cytoplasmic localization observed in TGF- β_1 -stimulated DFs. Therefore,

these findings supported the presence of defective lysosomal/endosomal activities in CWFs, potentially causing the abrogated sorting, transport, and degradation of lipids, proteins, and extracellular components, to and from the plasma membrane [37–40]. In addition to HA, it is well-established that HAS1 can be localized to the cellular endosome compartments and the plasma membrane, with endosomal HAS1 proposed to be involved in HA endocytosis for degradation or the regulation of HA synthesis at the endosomal membrane [62,63]. HAS1 can also interact with lysosomes, involved in HA degradation. Similarly, HAS2 is commonly localized at the endoplasmic reticulum, Golgi, and plasma membrane, in addition to being trafficked to endosomes and to the lysosomes for degradation, which such events being regulated via post-translational modifications, such as monoubiquitination or O-GlcNAcylation [62,63]. As such processes ultimately dictate HA levels through controlled synthesis and catabolism, the defective lysosomal/endosomal activities in CWFs, coupled with their prominent perinuclear HAS1 and HAS2 localization, could negatively impact on HA synthesis in CWFs overall. Indeed, as lysosomal, and endosomal dysfunctions associated with cellular ageing and senescence have been reported previously [64,65], it is plausible that similar events may be occurring in CWFs leading to altered lysosomal and endosomal trafficking and turnover of HA.

Impaired CWF wound healing capabilities, such as proliferation, migration, and growth factor responsiveness, are largely attributed to increased senescent CWF populations in chronic wounds induced via telomere-dependent (replicative senescent) or -independent (stress-induced, premature senescent) mechanisms [10–15]. Despite the contrasting PD and morphological differences indicative of increased CWF susceptibility to senescence identified herein, whether similar early-onset senescence changes contribute to such deleterious effects on CWF-myofibroblast differentiation remain to be fully established, facilitated through the more comprehensive analysis of additional senescence-related markers, such as SA- β -galactosidase activity and p53, p16^{INK4a} and p21^{waf1} expression. Nonetheless, now that the putative mechanisms underlying impaired TGF- β_1 -induced myofibroblast formation in CWFs have been identified herein, albeit in a limited number of CWF populations, further studies can investigate the relationship between these abrogated mechanisms versus the senescence status of CWFs derived from a wider range of chronic wound types, with contrasting wound durations and other patient donor characteristics. Similarly, we intend to undertake complementary studies to compare CWF-myofibroblast responses versus fibroblasts derived from acute healing wounds, to verify that the impaired mechanism we have identified are specific to cellular changes manifested within chronic wound environments alone. Additionally, as the abolition of HA pericellular coats and downregulated CD44/EGFR gene expression leads to reduced ERK1/2 signalling in TGF- β_1 -treated, aged DFs [24,25,28], further studies will assess the impact of disturbances to the non-classical HA/CD44/EGFR pathway on downstream p-ERK1/2 activation; and it's subsequent impact on TGF- β_1 -driven, myofibroblast differentiation in CWFs.

Therefore, in summary, as established with their inherent proliferative and migratory responses, this study has demonstrated that in contrast to DFs, TGF- β_1 -driven fibroblast-myofibroblast differentiation is severely impaired in venous ulcer- and pressure sore-derived CWFs, concomitant with defective lysosomal/endosomal activities and driven by dysfunctional activation of the non-classical HA/CD44/EGFR pathway. Irrespective of wound type, CWFs exhibited common alterations in HAS1 and HAS2 expression and perinuclear localization profiles, coupled with deregulated hyaladherin (CD44, TSG-6, and I α I heavy chain motifs, HC3, HC4 and HC5) induction following TGF- β_1 stimulation, which led to attenuated HA pericellular coat formation and reduced CD44/EGFR co-localization within membrane lipid rafts, essential for myofibroblast phenotype development. The identification of such disruptions to normal myofibroblast differentiation in CWFs, may lead to the development of new therapies aimed at restoring these

mechanisms and other established impairments to wound healing response in CWFs, in future.

CRediT authorship contribution statement

Nathaniel Glyn Morris: Writing – review & editing, Validation, Investigation, Formal analysis, Data curation. **Emma Louise Woods:** Writing – review & editing, Writing – original draft, Supervision, Methodology. **Jordanna Dally:** Writing – review & editing, Software, Methodology. **Adam Christopher Midgley:** Writing – review & editing, Supervision, Software, Methodology, Investigation. **Robert Steadman:** Writing – review & editing, Writing – original draft, Supervision, Resources, Project administration, Funding acquisition, Conceptualization. **Ryan Moseley:** Writing – review & editing, Writing – original draft, Supervision, Resources, Project administration, Funding acquisition, Conceptualization.

Funding

This study was supported by a PhD Studentship awarded by Health and Care Research Wales, Welsh Assembly Government, Cardiff, UK.

Declaration of competing interest

The authors declare that they have no known competing financial interests or personal relationships that could have appeared to influence the work reported in this paper.

Appendix B. Supplementary data

Supplementary data to this article can be found online at <https://doi.org/10.1016/j.yexcr.2025.114646>.

Data availability

Data will be made available on request.

References

- [1] E. Makrantonaki, M. Wlaschek, K. Scharffetter-Kochanek, Pathogenesis of wound healing disorders in the elderly, *J. Dtsch. Dermatol. Ges.* 15 (2017) 255–275.
- [2] J.F. Guest, N. Ayoub, T. McIlwraith, I. Uchegbu, A. Gerrish, D. Weidlich, K. Vowden, P. Vowden, Health economic burden that wounds impose on the National Health Service in the UK, *BMJ Open* 5 (2015) e009283.
- [3] J.F. Guest, G.W. Fuller, P. Vowden, Cohort study evaluating the burden of wounds to the UK's National Health Service in 2017/2018: update from 2012/2013, *BMJ Open* 10 (2020) e045253.
- [4] C.K. Sen, Human wound and its burden: updated 2020 compendium of estimates, *Adv. Wound Care (New Rochelle)* 10 (2021) 2812–2892.
- [5] M. Wlaschek, K. Scharffetter-Kochanek, Oxidative stress in chronic venous leg ulcers, *Wound Repair Regen.* 13 (2005) 452–461.
- [6] S.A. Eming, T. Krieg, J.M. Davidson, Inflammation in wound repair: molecular and cellular mechanisms, *J. Invest. Dermatol.* 127 (2007) 514–525.
- [7] I. Pastar, O. Stojadinovic, N.C. Yin, H. Ramirez, A.G. Nusbaum, A. Sawaya, S. B. Patel, L. Khalid, R.R. Isseroff, M. Tomic-Canic, Epithelialization in wound healing: a comprehensive review, *Adv. Wound Care (New Rochelle)* 3 (2014) 445–464.
- [8] S.M. Clayton, S.H. Shafikhani, A.M. Soulika, Macrophage and neutrophil dysfunction in diabetic wounds, *Adv. Wound Care (New Rochelle)* 13 (2024) 463–484.
- [9] A. Uberoi, A. McCready-Vangi, E.A. Grice, The wound microbiota: microbial mechanisms of impaired wound healing and infection, *Nat. Rev. Microbiol.* 22 (2024) 507–521.
- [10] M.V. Mendez, A. Stanley, H.Y. Park, K. Shon, T. Phillips, J.O. Menzoian, Fibroblasts cultured from venous ulcers display cellular characteristics of senescence, *J. Vasc. Surg.* 28 (1998) 876–883.
- [11] B.C. Kim, H.T. Kim, S.H. Park, J.S. Cha, T. Yufit, S.J. Kim, V. Falanga, Fibroblasts from chronic wounds show altered TGF- β -signaling and decreased TGF- β type II receptor expression, *J. Cell. Physiol.* 195 (2003) 331–336.
- [12] J.S. Vande Berg, M.A. Rose, P.L. Haywood-Reid, R. Rudolph, W.G. Payne, M. C. Robson, Cultured pressure ulcer fibroblasts show replicative senescence with elevated production of plasmin, plasminogen activator inhibitor-1, and transforming growth factor- β_1 , *Wound Repair Regen.* 13 (2005) 76–83.
- [13] I.B. Wall, R. Moseley, D.M. Baird, D. Kipling, P. Giles, I. Laffafian, P.E. Price, D. W. Thomas, P. Stephens, Fibroblast dysfunction is a key factor in the non-healing of chronic venous leg ulcers, *J. Invest. Dermatol.* 128 (2008) 2526–2540.
- [14] D. Jiang, J.C. de Vries, J. Muschhammer, S. Schatz, H. Ye, T. Hein, M. Fidan, V. S. Romanov, Y. Rinkevich, K. Scharffetter-Kochanek, Local and transient inhibition of p21 expression ameliorates age-related delayed wound healing, *Wound Repair Regen.* 28 (2020) 49–60.
- [15] R.J.R. Samdavid Thanapaul, M. Shvedova, G.H. Shin, J. Crouch, D.S. Roh, Elevated skin senescence in young mice causes delayed wound healing, *Geroscience* 44 (2022) 1871–1878.
- [16] Y. Tai, E.L. Woods, J. Dally, D. Kong, R. Steadman, R. Moseley, A.C. Midgley, Myofibroblasts: function, formation, and scope of molecular therapies for skin fibrosis, *Biomolecules* 11 (2021) 1095.
- [17] F.S. Younesi, A.E. Miller, T.H. Barker, F.M.V. Rossi, B. Hinz, Fibroblast and myofibroblast activation in normal tissue repair and fibrosis, *Nat. Rev. Mol. Cell Biol.* 25 (2024) 617–638.
- [18] N. Alizadeh, M.S. Pepper, A. Modarressi, K. Alfio, K. Schlaudraff, D. Montandon, G. Gabbiani, M.L. Bochaton-Piallat, B. Pittet, Persistent ischemia impairs myofibroblast development in wound granulation tissue: a new model of delayed wound healing, *Wound Repair Regen.* 15 (2007) 809–816.
- [19] A. Modarressi, G. Pietramaggiore, C. Godbout, E. Vigato, B. Pittet, B. Hinz, Hypoxia impairs skin myofibroblast differentiation and function, *J. Invest. Dermatol.* 130 (2010) 2818–2827.
- [20] K.M. McAndrews, T. Miyake, E.A. Ehsanipour, P.J. Kelly, L.M. Becker, D. J. McGrail, H. Sugimoto, V.S. LeBleu, Y. Ge, R. Kalluri, Dermal α SMA+ myofibroblasts orchestrate skin wound repair via β 1 integrin and independent of type I collagen production, *EMBO J.* 41 (2022) e109470.
- [21] X.M. Meng, D.J. Nikolic-Paterson, H.Y. Lan, TGF- β : the master regulator of fibrosis, *Nat. Rev. Nephrol.* 12 (2016) 325–338.
- [22] R.M. Simpson, S. Meran, D. Thomas, P. Stephens, T. Bowen, R. Steadman, A. Phillips, Age-related changes in pericellular hyaluronan organization leads to impaired dermal fibroblast to myofibroblast differentiation, *Am. J. Pathol.* 175 (2009) 1915–1928.
- [23] J. Webber, R.H. Jenkins, S. Meran, A. Phillips, R. Steadman, Modulation of TGF β 1-dependent myofibroblast differentiation by hyaluronan, *Am. J. Pathol.* 175 (2009) 148–160.
- [24] R.M. Simpson, A. Wells, D. Thomas, P. Stephens, R. Steadman, A. Phillips, Aging fibroblasts resist phenotypic maturation because of impaired hyaluronan-dependent CD44/epidermal growth factor receptor signaling, *Am. J. Pathol.* 176 (2010) 1215–1228.
- [25] A.C. Midgley, M. Rogers, M.B. Hallett, A. Clayton, T. Bowen, A.O. Phillips, R. Steadman, Transforming growth factor- β 1 (TGF- β 1)-stimulated fibroblast to myofibroblast differentiation is mediated by hyaluronan (HA)-facilitated epidermal growth factor receptor (EGFR) and CD44 co-localization in lipid rafts, *J. Biol. Chem.* 288 (2013) 14824–14838.
- [26] J., A. Martin, S. Midgley, E. Meran, T. Woods, A.O. Bowen, R. Steadman Phillips, Tumor necrosis factor-stimulated gene 6 (TSG-6)-mediated interactions with the inter- α -inhibitor heavy chain 5 facilitate tumor growth factor β 1 (TGF β 1)-dependent fibroblast to myofibroblast differentiation, *J. Biol. Chem.* 291 (2016) 13789–13801.
- [27] S., D. Meran, P. Thomas, J. Stephens, T. Martin, A. Bowen, R. Steadman Phillips, Involvement of hyaluronan in regulation of fibroblast phenotype, *J. Biol. Chem.* 282 (2007) 25687–25697.
- [28] A.C. Midgley, T. Bowen, A.O. Phillips, R. Steadman, MicroRNA-7 inhibition rescues age-associated loss of epidermal growth factor receptor and hyaluronan-dependent differentiation in fibroblasts, *Aging Cell* 13 (2014) 235–244.
- [29] C. A. G. Midgley, Morris, A.O. Phillips, R. Steadman, 17 β -estradiol ameliorates age-associated loss of fibroblast function by attenuating IFN- γ /STAT1-dependent miR-7 upregulation, *Aging Cell* 15 (2016) 531–541.
- [30] M.A. Loots, E.N. Lamme, J.R. Mekkes, J.D. Bos, E. Middelkoop, Cultured fibroblasts from chronic diabetic wounds on the lower extremity (non-insulin-dependent diabetes mellitus) show disturbed proliferation, *Arch. Dermatol. Res.* 291 (1999) 93–99.
- [31] J.D. Raffetto, M.V. Mendez, B.J. Marien, H.R. Byers, T.J. Phillips, H.Y. Park, J. O. Menzoian, Changes in cellular motility and cytoskeletal actin in fibroblasts from patients with chronic venous insufficiency and in neonatal fibroblasts in the presence of chronic wound fluid, *J. Vasc. Surg.* 33 (2001) 1233–1241.
- [32] J.D. Raffetto, R. Vasquez, D.G. Goodwin, J.O. Menzoian, Mitogen-activated protein kinase pathway regulates cell proliferation in venous ulcer fibroblasts, *Vasc. Endovasc. Surg.* 40 (2006) 59–66.
- [33] C.C. Seah, T.J. Phillips, C.E. Howard, I.P. Panova, C.M. Hayes, A.S. Asandra, H.Y. J. Park, Chronic wound fluid suppresses proliferation of dermal fibroblasts through a Ras-mediated signaling pathway, *J. Invest. Dermatol.* 124 (2005) 466–474.
- [34] K.J. Livak, T.D. Schmittgen, Analysis of relative gene expression data using real-time quantitative PCR and the 2^{- $\Delta\Delta$ CT} method, *Methods* 25 (2001) 402–408.
- [35] R.H. Jenkins, G.J. Thomas, J.D. Williams, R. Steadman, Myofibroblastic differentiation leads to hyaluronan accumulation through reduced hyaluronan turnover, *J. Biol. Chem.* 279 (2004) 41453–41460.
- [36] A.C. Midgley, E.L. Woods, R.H. Jenkins, C. Brown, U. Khalid, R. Chavez, V. Hascall, R. Steadman, A.O. Phillips, S. Meran, Hyaluronidase-2 regulates RhoA signaling, myofibroblast contractility, and other key profibrotic myofibroblast functions, *Am. J. Pathol.* 190 (2020) 1236–1255.
- [37] P.C. Trivedi, J.J. Bartlett, T. Pulinilkunnil, Lysosomal biology and function: modern view of cellular debris bin, *Cells* 9 (2020) 1131.
- [38] İ. Meraş, J. Maes, S. Lefrancois, Mechanisms regulating the sorting of soluble lysosomal proteins, *Biosci. Rep.* 42 (2022) BSR20211856.

- [39] J. Gilleron, A. Zeigerer, Endosomal trafficking in metabolic homeostasis and diseases, *Nat. Rev. Endocrinol.* 19 (2023) 28–45.
- [40] R. Kamentseva, V. Kosheverova, M. Kharchenko, M. Zlobina, A. Salova, T. Belyaeva, N. Nikolsky, E. Kornilova, Functional cycle of EEA1-positive early endosome: direct evidence for pre-existing compartment of degradative pathway, *PLoS One* 15 (2020) e0232532.
- [41] D.S. Schwarz, M.D. Blower, The endoplasmic reticulum: structure, function and response to cellular signaling, *Cell. Mol. Life Sci.* 73 (2016) 79–94.
- [42] P. Kulkarni-Gosavi, C. Makhouli, P.A. Gleeson, Form and function of the Golgi apparatus: scaffolds, cytoskeleton and signalling, *FEBS Lett.* 593 (2019) 2289–2305.
- [43] Y. Zhang, V. Srivastava, B. Zhang, Mammalian cargo receptors for endoplasmic reticulum-to-Golgi transport: mechanisms and interactions, *Biochem. Soc. Trans.* 51 (2023) 971–981.
- [44] F. Boraldi, F.D. Lofaro, S. Bonacorsi, A. Mazzilli, M. Garcia-Fernandez, D. Quaglino, The role of fibroblasts in skin homeostasis and repair, *Biomedicines* 12 (2024) 1586.
- [45] K. Tominaga, H.I. Suzuki, TGF- β signaling in cellular senescence and aging-related pathology, *Int. J. Mol. Sci.* 20 (2019) 5002.
- [46] A. Hasan, H. Murata, A. Falabella, S. Ochoa, L. Zhou, E. Badiavas, V. Falanga, Dermal fibroblasts from venous ulcers are unresponsive to the action of transforming growth factor- β_1 , *J. Dermatol. Sci.* 16 (1997) 59–66.
- [47] L. Wu, Y.P. Xia, S.I. Roth, E. Gruskin, T.A. Mustoe, Transforming growth factor- β_1 fails to stimulate wound healing and impairs its signal transduction in an aged ischemic ulcer model: importance of oxygen and age, *Am. J. Pathol.* 154 (1999) 301–309.
- [48] G.J. Fisher, Y. Shao, T. He, Z. Qin, D. Perry, J.J. Voorhees, T. Quan, Reduction of fibroblast size/mechanical force down-regulates TGF- β type II receptor: implications for human skin aging, *Aging Cell* 15 (2016) 67–76.
- [49] Z. Qin, G.J. Fisher, J.J. Voorhees, T. Quan, Actin cytoskeleton assembly regulates collagen production via TGF- β type II receptor in human skin fibroblasts, *J. Cell Mol. Med.* 22 (2018) 4085–4096.
- [50] A.C. Pretrey, C.A. de la Motte, Hyaluronan, a crucial regulator of inflammation, *Front. Immunol.* 5 (2014) 101.
- [51] H. Siiskonen, S. Oikari, S. Pasonen-Seppänen, K. Rilla, Hyaluronan synthase 1: a mysterious enzyme with unexpected functions, *Front. Immunol.* 6 (2015) 43.
- [52] J.P. Pienimäki, K. Rilla, C. Fulop, R.K. Sironen, S. Karvinen, S. Pasonen, M. J. Lammi, R. Tammi, V.C. Hascall, M.I. Tammi, Epidermal growth factor activates hyaluronan synthase 2 in epidermal keratinocytes and increases pericellular and intracellular hyaluronan, *J. Biol. Chem.* 276 (2001) 20428–20435.
- [53] K. Rilla, S. Oikari, T.A. Jokela, J.M. Hyttinen, R. Kärnä, R.H. Tammi, M.I. Tammi, Hyaluronan synthase 1 (HAS1) requires higher cellular UDP-GlcNAc concentration than HAS2 and HAS3, *J. Biol. Chem.* 288 (2013) 5973–5983.
- [54] J.A. Mack, J. R. N. Feldman, K. Itano, M. Kimata, V.C. Lauer, E.V. Maytin Hascall, Enhanced inflammation and accelerated wound closure following tetraborborol ester application or full-thickness wounding in mice lacking hyaluronan synthases Has1 and Has3, *J. Invest. Dermatol.* 132 (2012) 198–207.
- [55] Y. Wang, J.A. Mack, V.C. Hascall, E.V. Maytin, Transforming growth factor- β receptor-mediated, p38 mitogen-activated protein kinase-dependent signaling drives enhanced myofibroblast differentiation during skin wound healing in mice lacking hyaluronan synthases 1 and 3, *Am. J. Pathol.* 192 (2022) 1683–1698.
- [56] S.P. Evanko, M.I. Tammi, R.H. Tammi, T.N. Wight, Hyaluronan-dependent pericellular matrix, *Adv. Drug Deliv. Rev.* 59 (2007) 1351–1365.
- [57] S. Shakya, J.A. Mack, M. Alipour, E.V. Maytin, Cutaneous wounds in mice lacking TSG-6 exhibit delayed closure and an abnormal inflammatory response, *J. Invest. Dermatol.* 140 (2020) 2505–2514.
- [58] H. Shiraha, K. Gupta, K. Drabik, A. Wells, Aging fibroblasts present reduced epidermal growth factor (EGF) responsiveness due to preferential loss of EGF receptors, *J. Biol. Chem.* 275 (2000) 19343–19351.
- [59] H. Siiskonen, R. Kärnä, J.M. Hyttinen, R.H. Tammi, M.I. Tammi, K. Rilla, Hyaluronan synthase 1 (HAS1) produces a cytokine- and glucose-inducible, CD44-dependent cell surface coat, *Exp. Cell Res.* 320 (2014) 153–163.
- [60] L. Matos, A.M. Gouveia, H. Almeida, ER stress response in human cellular models of senescence, *J. Gerontol. A Biol. Sci. Med. Sci.* 70 (2015) 924–935.
- [61] J. Despres, Y. Ramdani, M. di Giovanni, M. Bénard, A. Zahid, M. Montero-Hadjadje, F. Yvergnaux, T. Sagué, A. Driouich, M.L. Follet-Gueye, Replicative senescence of human dermal fibroblasts affects structural and functional aspects of the Golgi apparatus, *Exp. Dermatol.* 28 (2019) 922–932.
- [62] G. Bart, N.O. Vico, A. Hassinen, F.M. Pujol, A.J. Deen, A. Ruusala, R.H. Tammi, A. Squire, P. Heldin, S. Kellokumpu, M.I. Tammi, Fluorescence resonance energy transfer (FRET) and proximity ligation assays reveal functionally relevant homo- and heteromeric complexes among hyaluronan synthases HAS1, HAS2, and HAS3, *J. Biol. Chem.* 290 (2015) 11479–11490.
- [63] R.M. Melero-Fernandez de Mera, U.T. Arasu, R. Kärnä, S. Oikari, K. Rilla, D. Vigetti, A. Passi, P. Heldin, M.I. Tammi, A.J. Deen, Effects of mutations in the post-translational modification sites on the trafficking of hyaluronan synthase 2 (HAS2), *Matrix Biol.* 80 (2019) 85–103.
- [64] E.Y. Shin, N.K. Soung, M.A. Schwartz, E.G. Kim, Altered endocytosis in cellular senescence, *Ageing Res. Rev.* 68 (2021) 101332.
- [65] L. Guerrero-Navarro, P. Jansen-Dürr, M. Cavinato, Age-related lysosomal dysfunctions, *Cells* 11 (2022) 1977.